Local and Remote Estimations using Fitted Polynomials in Distribution Systems

Conor Murphy, *Member, IEEE* and Andrew Keane, *Senior Member, IEEE*

***Abstract*—This work describes a technique to define a single parametric equation that estimates remote conditions within a distribution network, in an online setting, without dedicated telemetry. In this novel approach, a departure from conventional state estimation is explored to facilitate a fully decentralized operation. Derived based on fundamental treatment of ac power flow, the electrical behavior of a section of network is defined to a tractable constraint space using regression analysis. In this non-iterative technique, a measurement set consisting of the local voltage magnitude, active and reactive power injections at a single node are the input to pre-computed polynomials. Remote current flow, active power and reactive power flow as well as remote and local voltages and sensitivities are estimated in a direct calculation from period to period. Accurate estimations are also found in the presence of transducer errors. To assess the applicability of this technique at differing voltage levels a range of reactance to resistance ratios are considered.**

***Index Terms*—Distributed estimation, energy resources, multi-variable functions, power distribution, voltage measurement**

I. Introduction

THE flow of current through power system infrastructure is contingent on the physical connection between multiple busbars and the locations of generation and demand. The voltage experienced at a node is the result of complex power injections at every node on the power system in a given instant. Altering the network topology, a transformer tap setting or the amount or location of demand or generation changes the characteristics of the ac power flow problem, leading to a new set of power flows and node voltages. This work asks; to what extent can the voltage measurement at a single node be used to estimate remote complex power flows and sensitivities, which result in that voltage? As distinct from state estimation techniques this work features a non-iterative calculation, and in an online setting does not require a communication medium.

State estimation is an established method that can infer the state of the power system from a limited measurement set and is used to assess the security and stability of the system [1]–[3]. To produce a satisfactory output requires that accurate measurements are communicated in good time, and requires an accurate representation of line parameters and topology. Usually, weighted least squares estimation is used to align what is known about the system to a scenario that is in agreement with available measurements. Though typically thought of as a calculation performed centrally, a distributed state estimation technique as presented in [4] would be advantageous to distribution system operators owing to the decrease in available measurements in that context. With increasing distributed generation (DG) and increased consumer flexibility, state estimation is continually being improved for use in wider adaptations [5]. On distribution systems, Muscas et al [6] identify the scarcity of measurement and monitoring devices and avail of overlapping measurements in defined areas to estimate the state of the network. Complementary to the state estimation technique, online grid impedance estimation [7]–[9] and online Thévenin equivalent estimation [10] are topics of growing interest and relevance to distributed control.

The variation in voltage sensitivities on the distribution network is a well-established observation in the literature; used implicitly in any work containing OPF techniques and explicitly in [11] as a means of optimally allocating generation on distribution networks, in [12] to simultaneously manage both voltage and thermal constraints and in [13] to inform a local optimization technique minimizing current flow. In the latter, the seemingly linear trend in voltage sensitivities over a wide range of operating points brought about from a non-linear calculation is further elucidated here.

Fitted polynomials have been shown to be useful in estimating the energy loss on a system as a function of the amount of demand and other key system parameters [14], [15]. This work investigates the use of fitted parametric equations to accurately estimate both *local* and *remote* distribution system conditions. This paper follows from earlier work that formed part of a patent [16]. Using the measurement set at a single node, the flows and voltages at other points in a network are calculated. In other words, measurements at one point are used to infer system conditions at another point in the network without a dedicated communication infrastructure. This capability may render redundant the communication medium implicit in an optimal power flow deployment and enhance the performance of existing decentralized control techniques and indeed future techniques envisioned for a smart grid.

Section II describes the requirements for such an observation to be made successfully. In Section III the estimation technique is assessed using a time series power flow. Section IV presents the technique with varying X/R ratios, emphasizing the extent to which the assumptions for diverse voltage levels hold. Section V concludes the findings with some thought given to future applications.

This material is based upon works supported by the Science Foundation Ireland and is funded through the SEES Cluster, under Grant No. SFI/09/SRC/E1780 and also Enterprise Ireland, under Grant No. CF/2013/3628 Smart Control of Wind Farms. Paper no. TPWRS- 00691-2016. The opinions, findings and conclusions or recommendations expressed in this material are those of the author(s) and do not necessarily reflect the views of the Science Foundation Ireland.

C. Murphy and A. Keane are with the School of Electrical and Electronic Engineering, University College Dublin, Dublin 4, Ireland; e-mail: conchur.o-murchu@ucdconnect.ie; andrew.keane@ucd.ie).

II. Methodology

In the proposed estimation approach, measurements at a single node are substituted into polynomials that, when solved, provide an estimate for *remote* flows on the network as well as *local* and *remote* voltages and sensitivities. Treatment of the ac power flow problem is required in initial offline network studies to determine system characteristics, thereafter no communication is assumed. Using the necessary observations obtained from these studies at a known operating point, measurements at a single node are related to various system conditions of interest using regression analysis. The extrapolation of these planes to track the variability of these equations across multiple operating points is explained.

A. Determination of System Characteristics

Determining the system characteristics in the present approach requires the solution of the ac power flow problem. Assuming the general π-equivalent circuit for every branch and node pair, known series admittances; g_{ij} and b_{ij}, and shunt admittances; g_{si} and b_{si}, are used to form the admittance matrix of the network. For transformers, assuming the appropriate transformations are performed, a leakage impedance and magnetizing impedance can be included in the relevant entries of the admittance matrix, [17]. A recalculation of their effective admittance is necessary in the case of a change in tap position, modelled in this work as per [18] .

A matrix of sensitivities emerges from the convergence of the power flow problem, describing the relationship between polar node voltages and complex power injections (1).

$$\begin{bmatrix} \triangle P_1 \\ \triangle Q_1 \\ \vdots \\ \triangle P_i \\ \triangle Q_i \end{bmatrix} = \begin{bmatrix} \frac{\partial P_1}{\partial \theta_1} & \frac{\partial P_1}{\partial |V_1|} & \cdots \\ \frac{\partial Q_1}{\partial \theta_1} & \frac{\partial Q_1}{\partial |V_1|} & \cdots \\ \vdots & \vdots & \ddots \end{bmatrix} \cdot \begin{bmatrix} \triangle \theta_1 \\ \triangle |V_1| \\ \vdots \\ \triangle \theta_j \\ \triangle |V_j| \end{bmatrix} \quad (1)$$

This Jacobian matrix encapsulates the sensitivity of the power system at the point of convergence, and describes the change in voltage angle and voltage magnitude that would occur at a given node due to the injection of active power or reactive power at any other node. The calculation of the matrix varies between diagonal and off-diagonal entries; a full treatment of these equations can be found in [19]. Using an unbalanced ac power flow in the offline procedure extends the application to estimating unbalanced distribution networks. The technique does not specifically require the solution to the balanced Newton-Raphson power flow, other solutions to the power flow problem can be used such as the unbalanced four-conductor current injection method [20]. With a converged solution in hand, where the error function is reduced to an acceptably small tolerance, the node voltage angle and magnitude solutions combined with the series and shunt admittances are used to equate the complex power flow on each branch of the system; active power P and reactive power Q flow on any branch ij is calculated from (2) and (3).

$$Pij = V_i^2(g_{si} + g_{ij}) - V_iV_j(g_{ij}cos\theta_{ij} + b_{ij}sin\theta_{ij}) \quad (2)$$

$$Qij = -V_i^2(b_{si} + b_{ij}) - V_iV_j(g_{ij}sin\theta_{ij} + b_{ij}cos\theta_{ij}) \quad (3)$$

Expanding on equations (2) and (3) the current flowing into a given line is calculated from (4) using the voltage magnitude V at this starting point, i.

$$|I_{ij}| = \frac{\sqrt{P_{ij}^2 + Q_{ij}^2}}{V_i} \quad (4)$$

This work hypothesizes that embedded characteristics of the non-linear ac power flow model can be represented by an expression with independent terms, evaluated using measurements from one point in a network. The analysis is undertaken in the context of a distribution network from the point of view of a single node, herein called the measurement node, with both active power and reactive power capability, i.e. a demand node or a node with generation. Crucially the demand level on the system is maintained to a single operating condition for this part of the analysis. Fig. 1 summarizes the data capturing phase to determine the system characteristics in a brute force manner. To capture the interdependence between multiple measurement nodes the formulation of equations are calculated in the same analysis.

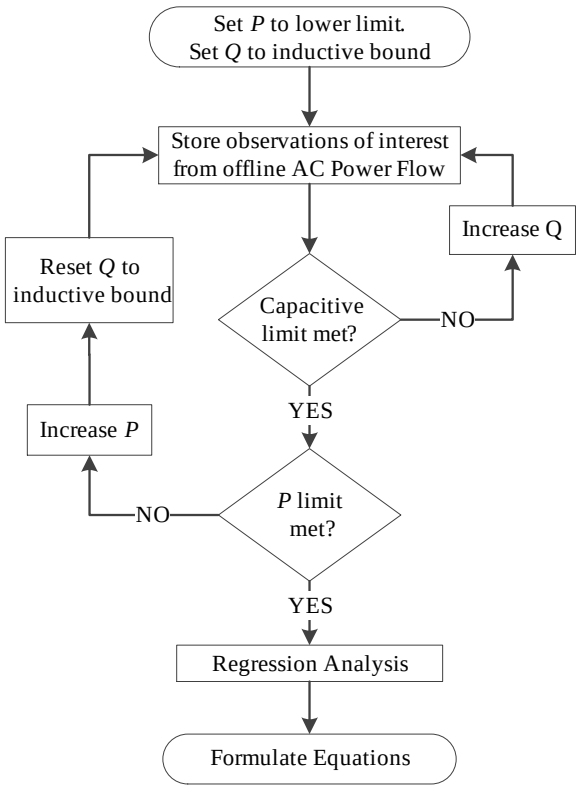

Fig. 1. Offline procedure to determine the system characteristics

At the measurement node(s), active power is set to the lower bound of operation, and reactive power is set to the lower inductive bound. An ac power flow is solved and the variables of interest are stored; these can include branch flows, (2 - 4), node voltages, and entries of the Jacobian matrix

(1). Next, a step change increase in reactive power occurs at the measurement node(s), in this instance a third of the upper capacitive limit. Individual power flows are solved until the measurement node(s) reach an upper capacitive bound. When all permutations of reactive power combinations have been captured, the active power at the measurement node(s) is increased, in this approach by 1%, and the procedure begins again; resetting the reactive power to the inductive bound, running a power flow at each reactive power set point and storing the results of interest from the converged power flow solutions. The granularity of step changes to active and reactive power are not limited to these values. This collection of observed *local* and *remote* operating points, found from all permutations of power injections at the measurement node(s), is now further analyzed. A non-linear regression analysis is undertaken that formulates the system characteristics of interest to the measurement set of voltage, V, active power, P and reactive power, Q at the measurement node(s) under investigation.

B. The Parametric Equations

In nonlinear regression, observational data can be modeled by a function containing a nonlinear combination of multiple independent variables. From the data captured using the procedure of Fig. 1, an equation can be formed using the local measurements at each node as the independent variables and the acquired data sets as the observable data. These equations estimate both local and remote conditions.

Least squares estimation minimizes the sum of square of residuals between the data and the evaluation of the fitted equations at respective points. An algorithm, for example the Gauss-Newton method, determines the shaping coefficients (x, y, z) of the fitted polynomial; beginning from an initial guess and converging toward a specified tolerance, moving the coefficients in a direction that minimizes the sum of squares of residuals [21]. This analysis is readily programmable as per [21] or in Matlab [22] using the function *nlinfit*. In this work, the chosen formulations are two-variable second-order equations linking local measurements of a node to desired observations. This requires that six shaping coefficients be determined from the regression analysis.

For a two variable equation of l and k, the following procedure applies. If n is the degree in l and m is the degree in k, the total degree of the polynomial is the maximum of n and m. The degree of l in each term is less than or equal to n, and the degree of k in each term is less than or equal to m. The total degree of any term in the polynomial cannot exceed the maximum of n and m [22]. The order of these polynomials can increase to allow for a more accurate formulation of the surface plots and more independent terms can be accommodated should the goodness of fit be unsatisfactory, however these formulations would require more coefficients. Rather than fixing the data to a two variable second order equation, an application of Cholesky decomposition [21] leaves the number of independent terms and the order of the polynomial as a free variable in the regression analysis; formulating the conditions whereby the shaping coefficients of a generic equation are determined. Further details on this formulation can be found in [23].

The system characteristics of interest to this work are current magnitude, active power and reactive power flows on remote lines, local voltage sensitivities and, vitally, the expected voltage at the demand level assumed in the analysis of Fig. 1. The representation of these characteristics are now contained in just six known coefficients per equation.

In (5) local measurements of active power, P, and voltage magnitude, V, at the terminals of a demand customer or generator are used to infer an estimate for current flow and flows of active power and reactive power on specified lines ij of the distribution network. These equations, each with unique coefficients x_{1-6}, are formed from the calculation of (2 - 4) in the power flow simulations of Fig. 1.

$$|I_{ij}|/P_{ij}/Q_{ij} = x_1P^2+x_2P+x_3PV+x_4V+x_5V^2+x_6 \quad (5)$$

Using the local node voltage magnitude and the reactive power measurement, Q, in (6), an estimate for the reactive power voltage sensitivity is analytically obtained. This formulation is obtained by observing the respective diagonal entries of the Jacobian matrix (1) in the procedure of Fig. 1. To reaffirm, active power voltage sensitivities and angle sensitivities can also be formulated in this manner, although the active power measurement is a better metric in these cases.

$$\frac{\partial Q_i}{\partial V_j} = y_1Q^2 + y_2Q + y_3QV + y_4V + y_5V^2 + y_6 \quad (6)$$

Inaccurate representation of system parameters and changes to system parameters, such as line reconfiguration, will affect the accuracy of the estimation technique. System parameters should be modelled as accurately as possible and reflect actual system values. In the case of reconfiguration, the new configuration can also be represented by new, separately defined, shaping coefficients. To obtain accurate estimations in the event of a reconfiguration requires online updating of the shaping coefficients and for the new configuration to be analyzed in the procedure outlined in Fig. 1. In the case of radial networks all *backfeed* configurations are known, so this analysis can be performed a proiri.

C. Interpreting for a Change in Demand

Unaccounted for, as yet, is the influence changing demand will have on these estimations. A change in demand will influence the voltage at each measurement location in a different manner, dependent on the change in active power, possible shifts in the power factor and the diversity in demand from location to location. To extrapolate the analysis outside the time of assumed known demand, (7) relates the active power, P, and reactive power, Q, of the measurement node to its local voltage magnitude, V_m, at this demand level.

$$V_m^{Calc} = z_1P^2 + z_2P + z_3PQ + z_4Q + z_5Q^2 + z_6 \quad (7)$$

The procedure to correct for the presence of demand is to repeat the analysis in Fig. 1 at another demand level. The

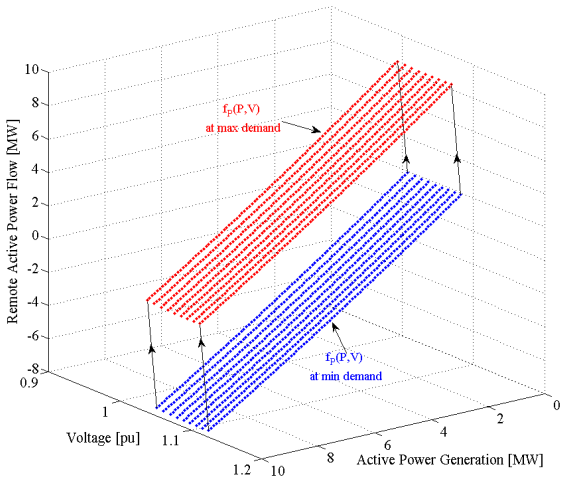

Fig. 2. Remote active power flow as a function of local voltage magnitude (V) and active power generation (P)

difference in coefficients of (7) of the two demand levels z_{1-6} are used to calculate a set of known slopes between the respective differences in coefficients of the other defined equations x_{1-6} and y_{1-6}. Using these slopes in the presence of unknown demand levels, the error between (7) and the measured voltage is used to interpolate or extrapolate the value of these coefficients to match the demand level. Fig. 2 illustrates an example of the interpolation procedure for remote active power flows. Shown on the figure are the extremes of active power flows resulting from expected maximum and minimum demand conditions for all combinations of active and reactive power set points and resulting voltage magnitudes. Not altering the shaping coefficients of Equations (5) in the presence of demand, will result in an inaccurate estimation of remote flows; where the inputs of voltage and active power calculate differing estimates to reality.

D. Application of Method

In calculating the polynomials (5 - 7) from all possible combinations of active power and reactive power at the measurement node, they can now be used at the location of the measurement set to estimate: line flows on *remote* feeders, both *remote* and *local* node voltages, as well as a range of voltage sensitivities. Put simply, from one measurement node a complete picture of the feeders in the vicinity is built, represented by unique shaping coefficients of the formulated polynomials.

In essence, these parametric equations are an accurate representation of the system characteristics in a given instant. In defining these characteristics to a single equation the solution space of these observations will exist on a single plane, making a direct calculation possible. These polynomials only require the measurement set of a single node, namely the voltage magnitude and the set-points of active power and reactive power. Implementation of the method enables a decentralized control procedure, where this non-iterative calculation is performed in a given time-step, to estimate remote conditions and potentially inform a new control regime.

TABLE I
TEST CASE NETWORK DATA

Node	Voltage [kV]	WF Cap. [MW]	Line	R [Ω]	X [Ω]
00	110	-	0102	5.45	5.72
01	38	-	0105	2.45	2.62
02	38	-	0107	6.34	6.66
03	38	20	0203	4.09	4.37
04	38	-	0204	1.39	1.48
05	38	12	0506	5.64	6.01
06	38	-	0607	2.96	3.14
07	38	-	0708	11.34	11.92
08	38	4			

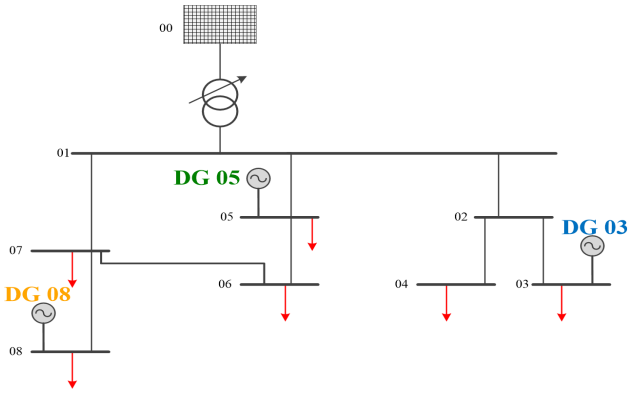

Fig. 3. Test network topology and location of demand and generation

III. TEST CASE

In order to validate this novel analytical approach the system characteristics of a section of existing Irish distribution system infrastructure are first established. Then in a simulation environment using time-series power flow, estimations are found from the direct calculation of equations (5 - 7) and compared against the true values. The test network under examination is a section of a distribution system with both radial and looped configurations, shown in Fig. 3. A 63 MVA transformer feeds the network rated at 38 kV from a transmission system at 110 kV modeled as an infinite bus. Three generators are embedded in the network, one on the radial section and two more on the looped section of network. Eight overhead lines make up this section of network that vary in length and exhibit X/R ratios of approximately one. The line parameters, DG capacities and rated voltage levels are provided in Table I. Characterization of a larger test network of 69 branches [24] has also been conducted, provided in Appendix A. Shaping coefficients and polynomials are obtained for each DG, however the technique is not exclusively applicable to these nodes alone; nodes without generation can also be used.

A. Network Characterization

In the procedure of Fig. 1 remote line current flows, flows of active power and reactive power, observed voltages and calculated sensitivities are captured. The regression analysis

TABLE II
EXAMPLE COEFFICIENTS OF BRANCH FLOW ESTIMATES AT DG 03

Estimate (5)	x_1	x_2	x_3	x_4	x_5	x_6
$\|I_{0102}\|$	0.01	0.99	-0.93	-181.16	86.66	94.77
P_{0102}	0.01	0.67	-1.61	-276.88	133.11	145.93
Q_{0102}	0.0005	1.04	-0.0898	-15.94	-63.94	85.78

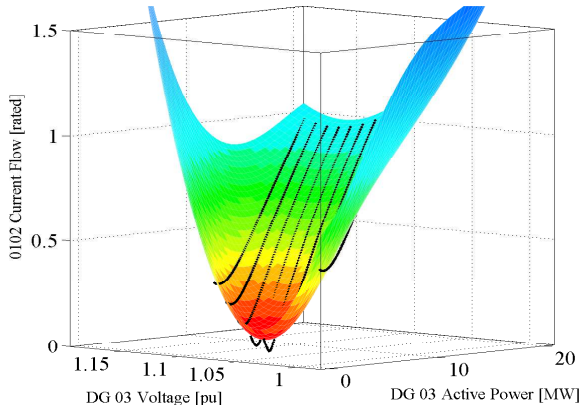

Fig. 4. Remote current flow of line 0102 shown as a function of active power and voltage of DG03

maps these observations as functions of the measurement voltage, active power and reactive power generation at each DG bus 03, 05 and 08. In the case of remote flows each DG takes observations of lines along the same feeder connection. So in the case of DG03 the measurement set of bus 03 is mapped against current flow, active power flow and reactive power flow on lines 0102, 0204 and 0203. DG05 estimates the same flows on line 0105 and 0506, and DG08 estimates flows on lines 0107, 0506, 0607 and 0708.

Shaping coefficients are determined through a regression analysis for each of the branch flows, formulating the estimate equations used in later sections. For example, recorded flow (current, active power and reactive power) of line 0102 from the analysis depicted in Fig. 1 are taken as the observed data or the dependent variable. The independent variables are taken as the recorded values of active power generation P of DG 03 and resulting voltage magnitude V at the terminals of DG 03 in the respective AC power flow solutions. The regression analysis then determines the best fit to the chosen formulation (5) using readily programmable equations of least squares regression, as per [21] or in Matlab using the *nlinfit* function. The values of three estimate equations' shaping coefficients are displayed in Table II for estimations local to DG 03.

In Fig. 4, one such observation and formulated surface is displayed; the line current flow on line 0102 against the calculated voltage and active power output of DG03. The current flow estimate, of the form (5), is displayed as a colored surface found from the regression analysis of the observed operating points displayed as black markers.

Fig. 5 shows the reactive power voltage sensitivity of bus 03 as a function of the calculated voltage and reactive power output of the DG03. As in [13] the sensitivities observed here

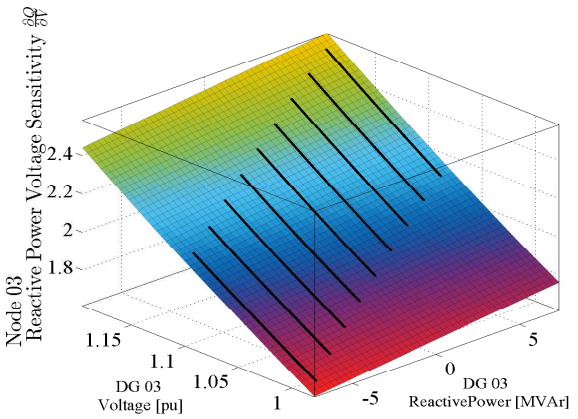

Fig. 5. Reactive power voltage sensitivity shown as a function of reactive power and voltage of DG03

over a wide range of operating conditions are seen to remain on the same plane when mapped. A non-linear calculation has produced a linear trend over all operating conditions of this DG and other DGs on the simulated system. This linear relationship also holds amongst the other entries of the Jacobian when mapped against the varying active and reactive power outputs available at the node.

1) Goodness of Fit: When using a regression analysis there a number of statistics that measure the goodness of fit of the formulated equation to the observed data, these are; the summed square of residuals error (SSE), the R^2 statistic and the Root Mean Squared Error (RMSE). A residual is the difference between the calculated estimate and the observed data. The better the fit, the closer the SSE will be to zero. The R^2 statistic measures how successful the fit is in explaining the variation of the data. The better the fit, the closer this number will be to one. The RMSE statistic is an estimate of the standard deviation of the random component in the data. The better the fit, the closer the RMSE number will be to zero. Table II displays the SSE in ascending order by type, along with the R^2 and RMSE for each estimate polynomial displayed alongside the measurement location.

The R^2 and RMSE results of each estimate polynomial (5 - 7) are an encouraging sign of the goodness of fit to the observed data. The SSE statistic of each polynomial also show promise, ranging from 26.46 to 1e-05 for polynomials of the form (5) that estimate current, active power and reactive power flow. The absolute values of current were observed in the offline procedure discounting for the change in direction of flows. In some instances, this leads to larger residual errors in the vicinity of low current flow when fitting a single equation to the data points in the regression analysis. Comparing the statistics from the expected voltages at each location (7), the radial section, V_{03}, has a better fit to its data than the data captured on the meshed loop configuration, V_{05} and V_{08}. Here DG05 is seen to influence the voltage measurements at DG08 and vice-versa; leading to an SSE and RMSE of up two orders of magnitude greater than the radial section. The estimates with the best fit are the reactive power voltage sensitivities

TABLE III
GOODNESS OF FIT OF THE ESTIMATE POLYNOMIALS

Estimate Parameter	Measurement Node	SSE	R^2	RMSE
$\lvert I_{0102}\rvert$ (5)	DG03	14.22	0.997	0.01397
$\lvert I_{0203}\rvert$ (5)	DG03	11.23	0.998	0.01241
$\lvert I_{0107}\rvert$ (5)	DG08	7.925	0.938	0.01043
$\lvert I_{0105}\rvert$ (5)	DG05	7.095	0.994	0.00986
$\lvert I_{0607}\rvert$ (5)	DG08	5.656	0.325	0.0081
$\lvert I_{0708}\rvert$ (5)	DG08	2.742	0.986	0.00613
$\lvert I_{0506}\rvert$ (5)	DG05	3.523	0.440	0.00695
$\lvert I_{0204}\rvert$ (5)	DG03	0.002	0.996	1e-06
P_{0107} (5)	DG08	26.46	0.9998	0.01905
P_{0506} (5)	DG05	20.69	0.8141	0.01685
P_{0105} (5)	DG05	14.05	0.9999	0.01413
P_{0102} (5)	DG03	6.305	1.000	0.00930
P_{0607} (5)	DG08	4.955	0.8816	0.00825
P_{0203} (5)	DG03	1.142	1.000	0.00396
P_{0708} (5)	DG08	0.418	1.000	0.00239
P_{0204} (5)	DG03	2e-05	0.7344	1e-05
Q_{0105} (5)	DG05	12.630	1.000	0.01316
Q_{0107} (5)	DG08	4.933	0.854	0.26020
Q_{0506} (5)	DG05	2.065	0.8619	0.0053
Q_{0203} (5)	DG03	1.865	1.000	0.00506
Q_{0607} (5)	DG08	0.974	0.8112	0.00366
Q_{0708} (5)	DG08	1.671	0.969	0.15140
Q_{0102} (5)	DG03	0.003	1.000	0.00058
Q_{0204} (5)	DG03	1e-05	0.7465	1e-05
V_{08} (7)	DG08	0.192	0.990	0.00162
V_{05} (7)	DG05	0.022	0.993	0.00055
V_{03} (7)	DG03	0.002	1.000	0.00015
$\partial Q_{03}/\partial V_{03}$ (6)	DG03	0.001	1.000	0.00012
$\partial Q_{05}/\partial V_{05}$ (6)	DG05	1e-04	0.993	0.00004
$\partial Q_{08}/\partial V_{08}$ (6)	DG08	1e-05	1.000	0.00001

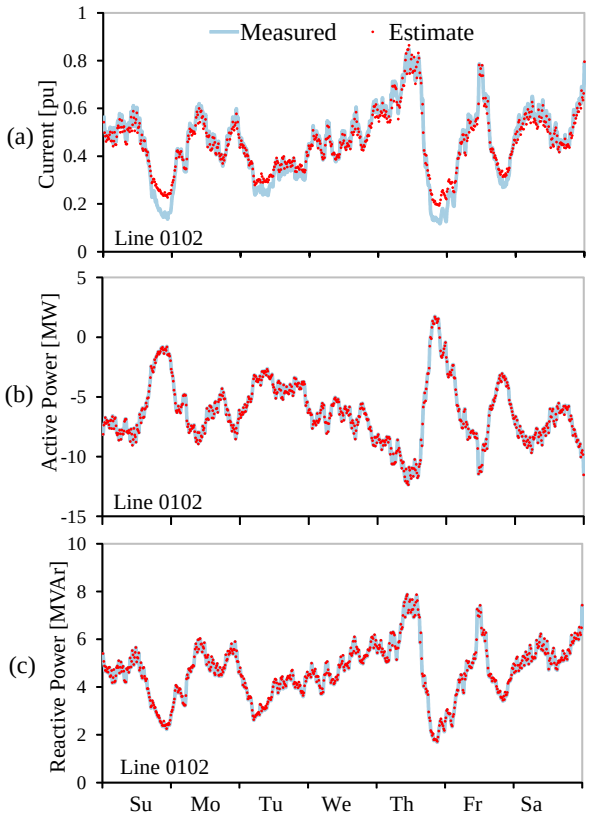

Fig. 6. Measured current (a), active power (b) and reactive power (c) flow on line 0102 shown alongside estimates from node 03 over time

(6), highlighting the potential for this estimate to be used in distributed control strategies, as in [13]. A true measure of the estimate performance can only be found in the presence of varying system conditions, as presented in the results of the time series power flow.

B. Time Series Power Flow Results

In a month long time series power flow with 15 minute resolution, demand and generation profiles are provided for each node in the network of Fig. 3. The generators operate with a constant power factor of 0.95 inductive. Using only measurements available at each DG, in each time-step the parameters listed in Table III are estimated in a direct calculation using the coefficients obtained from the network characterization procedure and the required measurement set.The mean execution time for an individual estimate polynomial to calculate its estimate from available measurements was calculated as 2 μs.

Taking the worst expected line current estimate based on the SSE results of Table III, Fig. 6 (a) shows the measured and estimate line current of line 0102 for the first week of the month. Also displayed in this plot are the resulting flows of active power (b) and reactive power (c), presented with the estimates made from DG03. These estimates use a polynomial of the form (5) and a measurement set consisting of active power generation and the voltage of node 03 available at the terminals of DG03. In all cases the estimate was shown to match well with the resultant flow. At low values for current flow the largest difference between measurement and estimate is evident, anticipated from the noticeable residual gap seen in Fig. 4. Here a precise estimate is less important than at times of high current flow, where the thermal limitation of the line could be breached. In contrast, in subplots, (b) and (c) a near exact match was made in every time step. Focusing on these promising results, Fig. 7 shows the active power and reactive power flow estimates and observations made for other formulated polynomials of (5).

The subplots of Fig. 7 (a) - (o) illustrate the estimate and resultant complex power, active power and reactive power flow for each of the lines. Also labeled on the scatter plots are the locations of estimation. An estimate with no error would appear on these plots at 45°, equidistant from both axes. Although not explicitly formulated with a polynomial, as seen, the estimation of complex power flow is possible by finding the root sum of squares of the active and reactive power estimates. In each of the subplots (a) to (o) the observations and estimates are in excellent agreement, tracking the ideally diagonal trend. The accuracy of these results and the fact that they are found from a direct calculation with no latency in communication, indicates the applicability for real time decentralized applications. Using these polynomials, local measurements could be used to sense congestion on remote parts of a network and inform a shift in the active and reactive power control regime.

Table III indicated that active power estimates of line 0107,

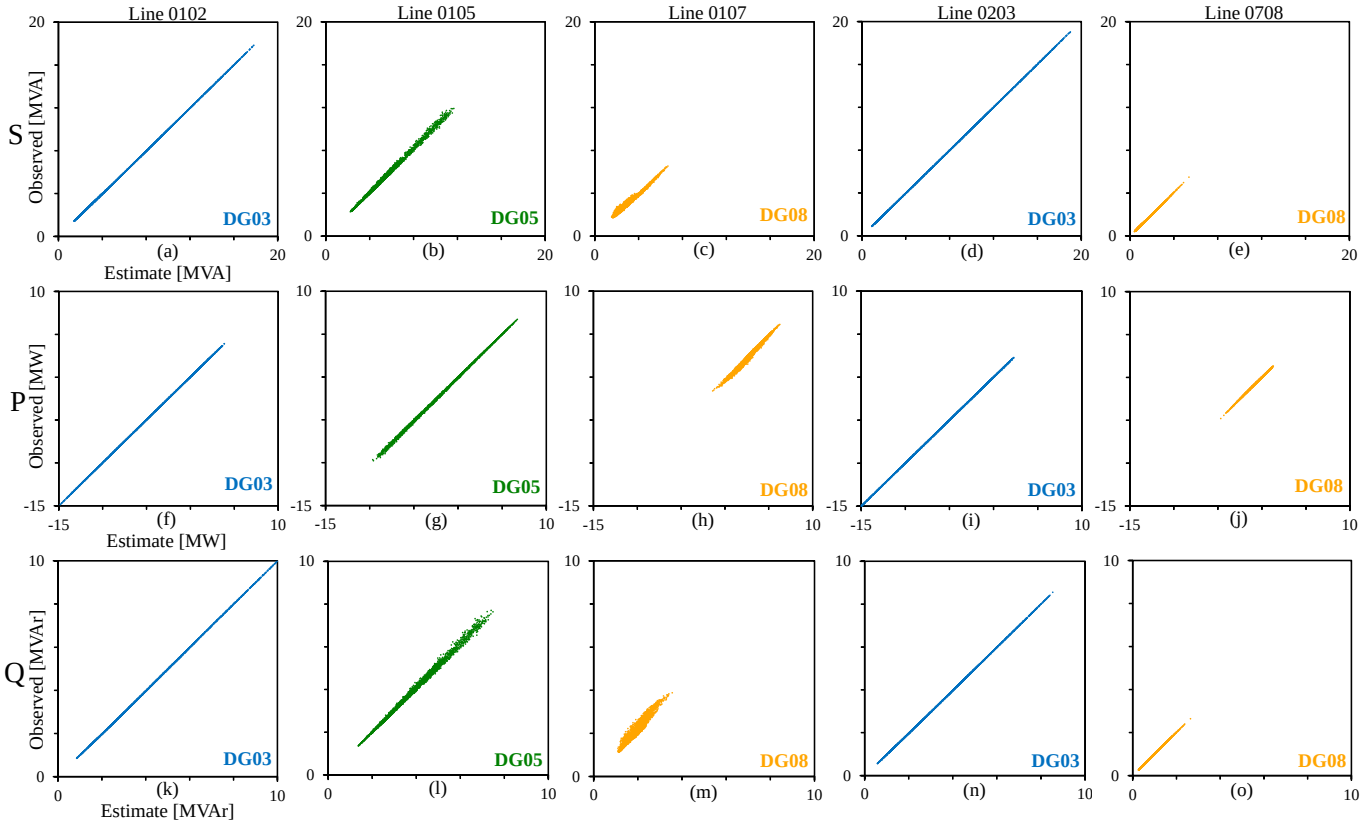

Fig. 7. Observed and estimate complex power (a)-(e), active power (f)-(j) and reactive power flow (k)-(o) on lines 0102, 0105, 0107, 0203 and 0708 shown with point of estimation based on month long time series power flow

Fig. 7 (h), from DG08 and reactive power estimates of line 0105, Fig. 7 (l), from DG 05 would be less accurate relative to the other power flow estimates. Estimates on these lines are affected by the interdependence of voltage sensitivities present on the looped network. In other words, demand at multiple locations and independent operating points of DG08 and DG05 affect the performance of the estimates. In these plots however, it was observed that the data points deviate only slightly from the ideally diagonal trend line, indicating that the procedure to interpret for a change in demand is working as expected.

In Table IV the mean absolute error, median error and standard deviation of the error is shown for each flow estimate considered (5), reactive power voltage sensitivities (6) and voltage estimates (7). The error in each case consists of the estimate of the parameter subtracted from the resultant recorded from the power flow simulation. Remote voltage estimates of non measurement nodes are presented in the table shown, having been also formulated with unique shaping coefficients in a polynomial of the form (5).

As seen in Table IV, the median value of all line current estimates is a negative number indicating that an overestimation occurs in these estimates. This is predominantly due to the anticipated overestimation at low values of current, ranging from 3 - 8.5% in this vicinity, as indicated by the residual gap seen in Fig. 4. However at times of peak line current the error reduces to 0.01% for all line estimates. The mean absolute error of active power flow ranges between 0.02 MW on line 0203 which experiences an average flow of -6 MW to 0.32 MW on line 0107 which has an average flow of 2.4 MW. For reactive power flow the mean absolute error ranges between 0.01 MVAr on line 0708 where the average flow was 0.9 MVAr to 0.22 MVAr on line 0107 which recorded 2.2

TABLE IV
MEAN, MEDIAN AND STANDARD DEVIATION OF THE ERROR

Estimate Parameter	Measurement Node	Mean	Median	Std. Dev.
I_{0102} [pu] (5)	DG03	0.0393	-0.0222	0.0408
I_{0105} [pu] (5)	DG05	0.0855	-0.0915	0.0401
I_{0107} [pu] (5)	DG08	0.0295	-0.0277	0.0206
I_{0203} [pu] (5)	DG03	0.0391	-0.0236	0.0415
I_{0708} [pu] (5)	DG08	0.0488	-0.0532	0.0211
P_{0102} [MW] (5)	DG03	0.0285	0.0278	0.0176
P_{0105} [MW] (5)	DG05	0.0970	-0.0642	0.1030
P_{0107} [MW] (5)	DG08	0.3196	-0.2883	0.1943
P_{0203} [MW] (5)	DG03	0.0171	-0.0027	0.0211
P_{0708} [MW] (5)	DG08	0.0248	0.0102	0.0300
Q_{0102} [MVAr] (5)	DG03	0.0248	-0.0251	0.0123
Q_{0105} [MVAr] (5)	DG05	0.0809	0.0356	0.0998
Q_{0107} [MVAr] (5)	DG08	0.219	0.1971	0.1715
Q_{0203} [MVAr] (5)	DG03	0.0248	-0.0253	0.0111
Q_{0708} [MVAr] (5)	DG08	0.0111	0.0076	0.0115
V_{02} [pu] (5)	DG03	0.0001	-0.0001	0.0001
V_{06} [pu] (5)	DG05	0.0014	0.0013	0.0010
V_{07} [pu] (5)	DG08	0.0004	0.0003	0.0003
V_{04} [pu] (5)	DG03	0.0001	-0.0001	0.0001
$\partial Q_3/\partial V_3$ (6)	DG03	0.00245	-0.00265	0.00127
$\partial Q_5/\partial V_5$ (6)	DG05	0.00184	-0.00172	0.00098
$\partial Q_8/\partial V_8$ (6)	DG08	0.00128	-0.00138	0.00066

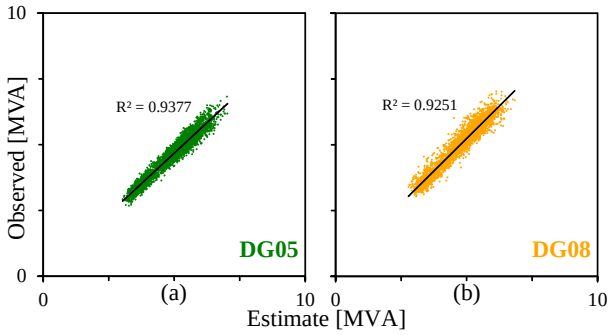

Fig. 8. Observed and estimate complex power on line 0506, as estimated from DG05 (a) and DG08 (b), shown with resulting R^2 statistics

MVAr on average. The results of the time series power flow confirmed that the promising indication from the goodness of fit observed in Table III, seen for the reactive power voltage sensitivities, proved true for estimating this parameter. The statistics of the error for this parameter are also shown in Table IV. In every time step considered, the estimate of the sensitivity strongly matched the result of the power flow.

In Fig. 8 one final comparison is shown, the observed and estimate complex power flow of line 0506. The flow of complex power in this line is influenced by independent demand at node 05, 06, 07 and 08, in addition to generation by units at node 05 and 08. Nonetheless, an accurate estimation for the complex flow is achieved by measurement node 05 and more remotely, node 08; both resulting in an R^2 above 0.92.

C. Comparative Tests with State Estimation

Whereas classic state estimation uses multiple measurements at numerous locations and an iterative technique to calculate the state of a section of network, the proposed method uses only the measurements at a single node to estimate the value of other nodal voltages and remote line flows that influence the voltage measurement at that node. The proposed methodology is a *fully*-decentralised *non*-iterative alternate approach to estimating system characteristics. Unique shaping coefficients of formulated polynomials need just three measurements to build a complete picture of the feeders in the vicinity, independent of network size. Thus the need for telemetry is greatly reduced, if required at all.

In a comparative test, the results of the time series power flow of part B are revisited in the context of state estimation. A state estimation procedure [25] is performed on the looped section of network of Fig. 3 using measurements with no error assumed. The minimum number of measurements required to ensure a comparatively accurate estimation of system flows for the looped section of network is eight, four voltage measurements at nodes 05, 06, 07 and 08 and the active and reactive power generation of DG 05 and 08.

As no measurement error was assumed, converged estimations resulted in an R^2 value of one when comparing resulting estimate flows to actual flows. Observability was not guaranteed in every time step however, of the 2881 periods considered 428 could not converge without input from further measurements, i.e. demand measurements at node 08 and 05. In contrast, using three measurements at node 08 in the proposed approach an estimate flow in every time-step was possible, with R^2 values ranging from 0.979 - 1 for the estimate complex power flows on this section of network.

TABLE V
COMPARISON OF R^2 STATISTICS WITH AND WITHOUT TRANSDUCER ERROR

Estimate Parameter	Measurement Node	R^2 with no error	R^2 with 2.5% error
S_{0102}	DG03	1.0000	0.9955
S_{0105}	DG05	0.9969	0.8229
S_{0107}	DG08	0.9796	0.8619
S_{0203}	DG03	1.0000	0.9983
S_{0708}	DG08	0.9995	0.9947
P_{0102} (5)	DG03	1.0000	0.9905
P_{0105} (5)	DG05	0.9996	0.8740
P_{0107} (5)	DG08	0.9876	0.9082
P_{0203} (5)	DG03	1.0000	0.9963
P_{0708} (5)	DG08	0.9994	0.9929
Q_{0102} (5)	DG03	1.0000	0.9955
Q_{0105} (5)	DG05	0.9963	0.8580
Q_{0107} (5)	DG08	0.9110	0.8127
Q_{0203} (5)	DG03	1.0000	0.9975
Q_{0708} (5)	DG08	0.9994	0.9931

1) Bad Data: The influence of measurement errors in state estimation necessitates the use of a bad data detection filter to avoid the detriment of estimate performance due to erroneous data. Measurement errors arise due to inaccurate transducer measurements and can be compounded with latency of communication to the central calculation. Meters may have biases, drifts or wrong connections which may cause larger measurement errors [18]. Reliable estimations are obtained through the identification and elimination of bad data at some measurement locations, aided by accurate readings at other locations [26], [27]. The proposed approach relies solely on three measurements at one location and all are required. Installing high-quality accurate transducers at the sole measurement location enables the detection of bad data from a simple plausibility check.

Telemetry failures, latency and noise from unexpected interference may also lead to large discrepancies between what is recorded and ultimately delivered to the central calculation of the classic state estimation technique. Owing to the elimination of telemetry, these factors do not influence estimates in the proposed local estimation technique.

D. Influence of Transducer Error

As there is no measurement redundancy, gross error elimination through practiced bad data analysis is not possible; this will compromise the accuracy of the estimates. To investigate the influence of a transducer error, the time series analysis is repeated with a random error added to the voltage measurements made at the terminals of the DG units. The random error is normally distributed with a range of 2.5% across the month long simulation. In this technique all estimates rely on a difference in voltage to tune the polynomial estimates to the observed demand level. For this reason an error in the voltage measurement is the worst conceivable for the proposed approach.

Shown in Table V are the experimentally found R^2 statistics of complex, active and reactive power flows from the time

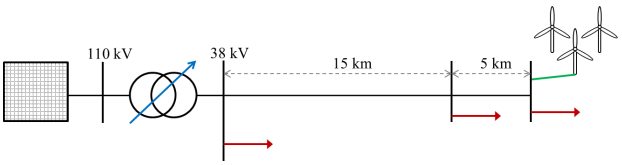

Fig. 9. 20 km radial test network with 20 MW DG unit

series power flow simulations shown with and without the random component of error. Unsurprisingly, a reduction in the performance of the estimates is observed when a transducer error is modeled. Whereas the R^2 ranged from 0.9110 to 1.000 in ideal conditions, the range expands to 0.8127 to 0.9975 with the inclusion of a transducer error. These findings indicate that the estimates retain sufficient accuracy, in the presence of standard transducer error, to be used in a decentralized control procedure.

IV. Influence of the X/R Ratio

To investigate if the novel approach of Section II holds for a wide range of X/R ratios a number of cable diameters are considered on a radial test network. A 20 MW wind farm resides at the end of a 20 km radial section of network as shown in Fig. 9. There are three load centers on this synthetic network, one located on the same busbar as the transformer secondary, another 5 km from the location of the DG, and lastly immediately adjacent to the location of generation. The conductor type of this 38 kV connection is modeled as an XLPE underground cable, with an X/R ratio increasing from 0.8 to 19.63. The series impedance and shunt admittance information for the different X/R ratios are available from [28].

The procedure to determine system characteristics Fig. 1 is repeated for 18 different cable diameters. In Fig. 10 reactive power voltage sensitivities as a function of known reactive power generation and local node voltage (6) is illustrated for each X/R ratio considered. In this figure the formulated surfaces are presented between four red guidelines indicating the direction of change of increasing X/R ratios.

The change in X/R ratio has the effect of moving the formulations of reactive power voltage sensitivities to new, distinctly tractable, values; illustrated as a vertical change in Fig. 10. Notably, the range of voltage values decreases with higher X/R ratios, signifying the dampened effect of voltage rise from active power injections. Also of note are the higher sensitivity values obtained at higher X/R ratios, in accordance with what one would intuitively expect for larger reactances.

Network topology reconfiguration is a typical occurrence on radial distribution feeders to ensure continuity of supply while scheduled maintenance is undertaken. The closing of a normally open point may add or subtract multiple km of cable to a network and this cable may be of different size and type to the cable now switched out, undoubtedly influencing the voltage sensitivities at the point of connection. This change will have the effect of moving the formulated surface of reactive power voltage sensitivities to new, distinctly tractable, values, as illustrated as a vertical change in Fig. 10. Changes in network configuration may be evident in the changes in

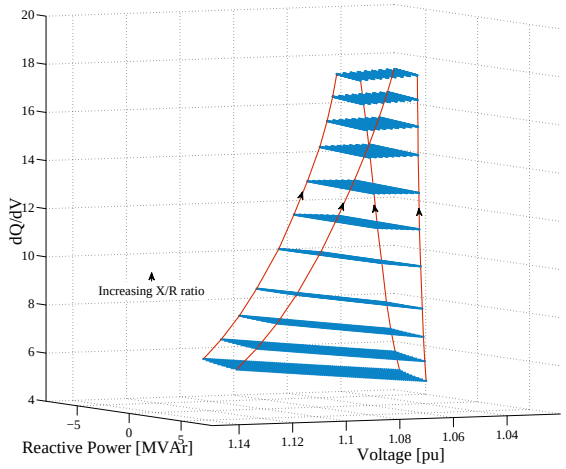

Fig. 10. Reactive power voltage sensitivities as a function of known reactive power generation and local node voltage for increasing X/R ratios

voltage resultant from the complex power regime of the unit from period to period.

V. Conclusion

Lack of observability on distribution systems will continue to challenge the operation of the power system, in particular with increased penetrations of distributed energy resources. Exploring the influence of a distributed energy resource on the ac power flow problem has revealed a highly accurate and effective decentralized estimation technique. The polynomials, defined here, analytically link remote system flows, remote and local voltages and sensitivities to a set of local measurements at the terminals of a distributed energy resource; namely voltage magnitude, active power and reactive power.

Once formulated from the regression analysis, the polynomials are solved non-iteratively in a direct calculation to provide an estimate of the desired *remote* and *local* system conditions. Allowing for the operation of an on-load tap-changer, changing demand and varying generation at multiple locations; line current flows, active and reactive power flows, remote voltages and voltage sensitivities are estimated in a time series power flow simulation with no communication medium. Repeating the network characterization technique over a wide range of X/R ratios and voltage levels has shown its applicability to a variety of networks.

Mapping remote system characteristics to a single equation confines the solution space to measurements within a tractable constraint space. Here, a direct calculation with no latency in communication gives an accurate estimate of system states, indicating the applicability for real time decentralized applications.

Appendix A
69-branch Distribution Feeder

The procedure of Section II is repeated for a network with 69 branches, illustrated in Fig. 11 found in [24]. DG units at node 20, 30, 40 and 50, estimate remote flows on lines 0405, 0328, 0436, 0447 respectively. Table VI displays the favorable statistics from the regression analysis for line current, active

TABLE VI
GOODNESS OF FIT AND PERFORMANCE OF THE ESTIMATE POLYNOMIALS

Estimate	Node	SSE	R^2	RMSE	Abs. Mean Err.	Time Series R^2
I_{0405} (5)	DG20	0.625	0.997	0.0095	0.085 [pu]	0.911
I_{0328} (5)	DG30	3.651	0.985	0.0231	0.019 [pu]	0.998
I_{0336} (5)	DG40	3.885	0.983	0.0238	0.006 [pu]	0.995
I_{0447} (5)	DG50	5.152	0.965	0.0274	0.027 [pu]	0.882
Q_{0405} (5)	DG20	0.0108	0.998	0.0013	0.039 [MVAr]	0.999
Q_{0328} (5)	DG30	0.1660	0.999	0.0049	0.028 [MVAr]	0.997
Q_{0336} (5)	DG40	0.1381	0.999	0.0045	0.009 [MVAr]	0.998
Q_{0447} (5)	DG50	0.0328	1.00	0.0022	0.002 [MVAr]	1.00
P_{0405} (5)	DG20	0.4997	0.997	0.0085	0.038 [MW]	0.996
P_{0328} (5)	DG30	0.00001	0.999	0.0001	0.003 [MW]	0.999
P_{0336} (5)	DG40	0.00001	0.999	0.0001	0.019 [MW]	0.999
P_{0447} (5)	DG50	0.00001	1.00	0.0001	0.001 [MW]	1.00

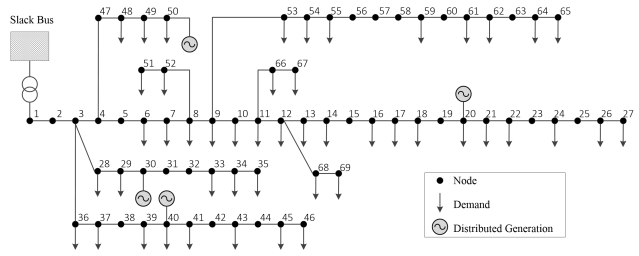

Fig. 11. 69 branch radial test network

and reactive power along these lines. A time series power flow, as per Section III, reveals close to unity R^2 values were determined from the observations and estimates.

ACKNOWLEDGEMENT

The authors would like to thank Dr. Peter Richardson for his interest and involvement in the completion of this work. This work was conducted in the Electricity Research Centre, University College Dublin, Ireland, which is supported by the Electricity Research Centres Industry Affiliates programme (http://erc.ucd.ie/industry/). The opinions, findings and conclusions or recommendations expressed in this material are those of the author(s) and do not necessarily reflect the views of the Science Foundation Ireland.

REFERENCES

[1] F. C. Schweppe and J. Wildes, "Power system static-state estimation, part I: Exact model," *IEEE Transactions on Power Apparatus and Systems*, vol. PAS-89, no. 1, pp. 120–125, Jan 1970.

[2] F. C. Schweppe and D. B. Rom, "Power system static-state estimation, part II: Approximate model," *IEEE Transactions on Power Apparatus and Systems*, vol. PAS-89, no. 1, pp. 125–130, Jan 1970.

[3] F. C. Schweppe, "Power system static-state estimation, part III: Implementation," *IEEE Transactions on Power Apparatus and Systems*, vol. PAS-89, no. 1, pp. 130–135, Jan 1970.

[4] V. Kekatos and G. Giannakis, "Distributed robust power system state estimation," *IEEE Trans. on Power Syst.*, vol. 28, no. 2, pp. 1617–1626, May 2013.

[5] A. Gomez-Exposito, A. Abur, A. de la Villa Jaen, and C. Gomez-Quiles, "A multilevel state estimation paradigm for smart grids," *Proceedings of the IEEE*, vol. 99, no. 6, pp. 952–976, June 2011.

[6] C. Muscas, M. Pau, P. Pegoraro, S. Sulis, F. Ponci, and A. Monti, "Multiarea distribution system state estimation," *IEEE Trans. Instrum. Meas*, vol. 64, no. 5, pp. 1140–1148, May 2015.

[7] H.-T. Yang, P.-C. Yang, and C.-L. Huang, "Evolutionary programming based economic dispatch for units with non-smooth fuel cost functions," *IEEE Trans. Power Syst.*, vol. 11, no. 1, pp. 112–118, 1996.

[8] L. Asiminoaei, R. Teodorescu, F. Blaabjerg, and U. Borup, "Implementation and test of on-line embedded grid impedance estimation for pv-inverters," in *Power Electronics Specialists Conference, 2004. IEEE 35th Annual*, vol. 4, 2004, pp. 3095–3101 Vol.4.

[9] M. Ciobotaru, R. Teodorescu, P. Rodriguez, A. Timbus, and F. Blaabjerg, "Online grid impedance estimation for single-phase grid-connected systems using pq variations," in *Power Electronics Specialists Conference, 2007. IEEE*, June 2007, pp. 2306–2312.

[10] S. Abdelkader and D. Morrow, "Online thevenin equivalent determination considering system side changes and measurement errors," *IEEE Trans. on Power Syst.*, vol. 30, no. 5, pp. 2716–2725, Sept 2015.

[11] A. Keane and M. O'Malley, "Optimal Allocation of Embedded Generation on Distribution Networks," *IEEE Trans. Power Syst.*, vol. 20, no. 3, pp. 1640–1646, 2005.

[12] T. Sansawatt, L. F. Ochoa, and G. P. Harrison, "Smart Decentralized Control of DG for Voltage and Thermal Constraint Management," *IEEE Trans. on Power Syst.*, vol. 27, no. 3, pp. 1637–1645, 2012.

[13] C. Murphy and A. Keane, "Optimised Voltage Control for Distributed Generation," in *PowerTech, 2015 IEEE Eindhoven*, 2015, pp. 1–6.

[14] M. Gustafson and J. Baylor, "Approximating the system losses equation," *IEEE Trans. on Power Syst.*, vol. 4, no. 3, pp. 850–855, Aug 1989.

[15] P. Rao and R. Deekshit, "Energy loss estimation in distribution feeders," *IEEE Trans. on Power Del.*, vol. 21, no. 3, pp. 1092–1100, July 2006.

[16] C. Murphy, A. Keane, and P. Richardson, "Method for Controlling Power Distribution," Irish Patent WO 2015/193 199 H02J 3/18, 2015.

[17] M. Thomson, "Automatic voltage control relays and embedded generation I," *Power Eng. Journal*, vol. 14, no. 2, pp. 71–76, April 2000.

[18] A. Abur and A. Gomez-Exposito, *Power System State Estimation: Theory and Implementation*. CRC Press, 2004.

[19] A. J. Wood and B. F. Wollenberg, *Power Generation, Operation, and Control*. J. Wiley & Sons, 1996.

[20] D. R. R. Penido, L. R. de Araujo, S. Carneiro, J. L. R. Pereira, and P. A. N. Garcia, "Three-phase power flow based on four-conductor current injection method for unbalanced distribution networks," *IEEE Transactions on Power Systems*, vol. 23, no. 2, pp. 494–503, May 2008.

[21] S. C. Chapra and R. P. Canale, *Numerical Methods for Engineers - 2nd Edition*. McGraw-Hill Book Company, 1988.

[22] MathWorks Inc., 2012. [Online]. Available: http://www.mathworks.com/

[23] A. Ralston and P. Rabinowitz, *A First Course in Numerical Analysis - International Series in Pure and Applied Mathematics*. McGraw-Hill Book Company, 1978.

[24] M. Baran and F. Wu, "Optimal capacitor placement on radial distribution systems," *IEEE Trans. on Power Del.*, vol. 4, no. 1, pp. 725–734, Jan 1989.

[25] J. Alber, "State estimation in PowerFactory: Algorithmic aspects," in *RTE-VT Workshop, Paris, France*, 2006.

[26] R. Doraiswami and J. L. R. Pereira, "A new bad data detection identification algorithm," *IEEE Transactions on Reliability*, vol. R-29, no. 4, pp. 333–335, Oct 1980.

[27] V. H. Quintana, A. Simoes-Costa, and M. Mier, "Bad data detection and identification techniques using estimation orthogonal methods," *IEEE Transactions on Power Apparatus and Systems*, vol. PAS-101, no. 9, pp. 3356–3364, Sept 1982.

[28] ABB, "XLPE Land Cable Systems; User's Guide," ABB, Tech. Rep., 2010. [Online]. Available: www.abb.com

Conor Murphy (S'13-M'16) received the B.Sc and M.E degrees in electrical engineering from University College Dublin, Dublin, Ireland, in 2011 and 2012, respectively. He is currently pursuing the Ph.D. degree in the School of Electrical and Electronic Engineering, University College Dublin, Dublin, Ireland. His research interests include the integration of distributed generation, reactive power control and AC optimal power flow.

Andrew Keane (S'04-M'07-SM'14) received the Ph.D. degree in electrical engineering from University College Dublin, Ireland in 2007. He is an Associate Professor and Head of the School of Electrical and Electronic Engineering, University College Dublin. He is also Head of the Energy Institute at UCD. He has previously worked with ESB Networks, the Irish Distribution System Operator. His research interests include power systems planning and operation, distributed energy resources, and distribution networks.